Calorimeters synchronization & energy binned fit at the Muon g-2 experiment

Roberto Ribatti

Università di Pisa, Scuola Normale Superiore

Supervisor: Marco Incagli

Abstract

In this report I summarize the work I have done at the Muon g-2 experiment during the Summer Internship at Fermilab. My work is divided into two distinct parts. In the first month I dealt with the timing calibration of the laser system in order to achieve the syncronization of all the 1296 crystals in the experiment. In the second month I performed a preliminary study of a new analysis technique, the energy binned wiggle fit, on the 60hr dataset.

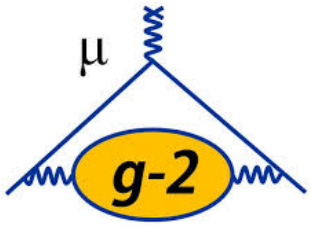

Fermilab

Contents

I. Introduction

The Muon g-2 Experiment E989 at Fermilab, has the main goal to measure the muon anomalous magnetic moment, $a_\mu = (g-2)/2$, to the unprecedented precision of 0.14 parts per million (ppm). This big experimental effort makes sense because:

- the Standard Model prediction for a_μ(Theo) is nowadays computed to similar precision: 0.42 ppm so the comparison between experiment and theory could provide a sensitive test of the model;
- the Brookhaven E821 experiment measured a_μ(Exp) to 0.54 ppm and this differs by 3.3 standard deviations from the SM prediction.

The BNL experiment was statistics limited so the storage ring was relocated to Fermilab where the Booster, the Recycler and the antiproton target station can be used to acquire a 20-fold increase in statistics to the new E989 experiment.

i. Physical context

For fermions the magnetic dipole moment $\vec{\mu}$ is related to the spin $\vec{s}$ by

$$\vec{\mu} = \frac{gQe}{2m}\vec{s}$$

One of the great successes of Dirac's relativistic theory was the prediction that $g \equiv 2$ but now we know that small deviation from this value arises from the radiative correction to the Dirac moment. It is useful to break the magnetic moment into two terms:

$$\mu = (1+a)\frac{e\hbar}{2m}$$

where $a = (g-2)/2$ is the anomalous (Pauli) moment.

ii. Sensitivity to new physics: electron vs. muon anomaly

Both the electron and muon anomalies have been measured very precisely [1]:

$$a_e(\text{Exp}) = 115965218073(28) \times 10^{-14} \qquad (\pm 0.24 \text{ ppb})$$
$$a_\mu(\text{Exp}) = 116592089(63) \times 10^{-11} \qquad (\pm 0.54 \text{ ppm})$$

While the electron anomaly has been measured to a much higher precision, less than a part per billion, it is significantly less sensitive to heavier physics, because the relative contribution of heavier virtual particles to the muon anomaly goes as $\left(\frac{m_\mu}{m_e}\right)^2 \simeq 43000$. Thus the lowest-order hadronic contribution to a_e is: $a_e^{had,LO} = (1.875 \pm 0.017) \times 10^{-12}$, which is 1.5 ppb of a_e. For the muon the hadronic contribution is 60 ppm (parts per million). So with much less precision, when compared with the electron, the measured muon anomaly is sensitive to mass scales in the several hundred GeV region.

iii. Experimental setting

Let's talk now about how practically the muon g-2 is measured at the E989 experiment. Polarized muons are produced and injected into the storage ring. The magnetic field is a dipole field, shimmed to ppm level uniformity. Vertical focusing is provided by electrostatic quadrupoles. Two frequencies are measured experimentally:

- the rate at which the muon polarization turns relative to the momentum, called ω_a;
- the value of the magnetic field normalized to the Larmor frequency of a free proton, ω_p.

The rate at which the spin turns relative to the momentum is $\vec{\omega_a} = \vec{\omega_S} - \vec{\omega_C}$, where S and C stand for spin and cyclotron. These two frequencies are given by

$$\begin{aligned}
\omega_S &= -g\frac{Qe}{2m}B - (1-\gamma)\frac{Qe}{\gamma m}B; \\
\omega_C &= -\frac{Qe}{m\gamma}B; \\
\omega_a &= \omega_S - \omega_C = -\left(\frac{g-2}{2}\right)\frac{Qe}{m}B = -a_\mu\frac{Qe}{m}B.
\end{aligned} \tag{1}$$

There are two important features of ω_a:

- it only depends on the anomaly rather than on the full magnetic moment;
- it depends linearly on the applied magnetic field.

In presence of an electrostatic field $\vec{E}$, Equation (1) becomes more complex:

$$\vec{\omega_a} = -\frac{Qe}{m}\left[a_\mu\vec{B} - \left(a_\mu - \left(\frac{mc}{p}\right)^2\right)\frac{\vec{\beta}\times\vec{E}}{c}\right]. \tag{2}$$

If operated at the "magic" momentum $p_{magic} = \frac{m}{\sqrt{a_\mu}} = 3.09$ GeV/c the electric field contribution cancels in first order, and requires a small correction in second order.

The reason for the use of the two frequencies (ω_a and ω_p), rather than the only ω_a and the magnetic field B can be understood from Equation (2): to obtain a_μ from this relation requires precise knowledge of the muon charge to mass ratio. To determine a_μ from the two frequencies ω_a and ω_p, we use:

$$a_\mu = \frac{\omega_a/\omega_p}{\lambda_+ - \omega_a/\omega_p} = \frac{\mathcal{R}}{\lambda_+ - \mathcal{R}}$$

where the ratio $\lambda_+ = \mu_{\mu^+}/\mu_p = 3.183345137(85)$ is the muon-to-proton magnetic moment ratio measured from muonium. Of course, to use λ_+ to determine a_{μ^-} requires the assumption of CPT invariance.

iv. Error Budget

Experience shows that many of the "known" systematic uncertainties can be addressed in advance and minimized, while other more subtle uncertainties appear only when the data is being analyzed. From the experience gained at the BNL E821 experiment it is expected that the Fermilab E989 experiment will have three main categories of uncertainties:

- **Statistical** The least-squares or maximum likelihood fits to the histograms describing decay positron events vs. time in the fill will determine ω_a, the anomalous precession frequency. The uncertainty $\delta\omega_a$ from the fits will be purely statistical (assuming a good fit). The final uncertainty depends on the size of the data set used in the fit, which in turn depends on the data accumulation rate and the running time. E989 must obtain 21 times the amount of data collected for E821. Using the T-method (for an explanation of this fitting method see Section III) to evaluate the uncertainty, 1.5×10^{11} events are required in the final fitted histogram to realize a 100 ppb statistical uncertainty. Various weighting schemes exist, beside the T-method, with different statistic power and sensitivity to systematics. A part of my work consisted in the preliminary study of a new kind of these fitting techniques in order to obtain better statistical power.

- ω_a **Systematics** Additional systematic uncertainties that will affect $\delta\omega_a$ might be anything that can cause the extracted value of ω_a from the fit to differ from the true value, beyond statistical fluctuations. Categories of concern include the detection system. (e.g., gain stability and pileup), the incoming beamline (lost muons, spin tracking), and the stored beam (coherent betatron oscillations, differential decay, E and pitch correction uncertainties). The target for this source of systematic uncertainty is to reach a $\pm$70 ppb to be compared with the 180 ppb level reached at E821. For a summary of the main source of error see Table 1. An other part of my work has the goal to reach a good time resolution which is a way to reduce two big source of error: pile-up and lost muons.
- ω_p **Systematics** The magnetic field is determined from proton NMR. The uncertainties are related to how well known are the individual steps from absolute calibration to the many stages of relative calibration and time-dependent monitoring. The "statistical" component to these measurements is negligible. Also for this source of systematic uncertainty, the goal is 70 ppb to be compared with the 170 ppb level reached at E821.

Category	E821 [ppb]	E989 Improvement Plans	Goal [ppb]
Gain changes	120	Better laser calibration	
		low-energy threshold	20
Pileup	80	Low-energy samples recorded	
		calorimeter segmentation	40
Lost muons	90	Better collimation in ring	20
CBO	70	Higher n value (frequency)	
		Better match of beamline to ring	< 30
E and pitch	50	Improved tracker	
		Precise storage ring simulations	30
Total	180	Quadrature sum	70

Table 1: *Error budget comparison for ω_a systematic between BNL and Fermilab experiment [1]*

II. Time synchronization of the calorimeters crystals

i. Introduction

A good time resolution is useful in order to minimize two big source of systematic error: pile-up and lost muons. Differently from the BNL experiment where calorimeters were unique crystals, the 24 calorimeters used in the E989 experiment consist of a 6x9 matrix of scintillator crystals[1] and a photo-detector (SiPM) for each crystal.
Each calorimeter has an independent read-out system in which SiPMs are read in group of 5 by 11 riders boards that digitize the waveform using a common clock for timing purpose[2]. The electronic connection between SiPMs and riders can be a little different for each photo-detector and there could be a common difference of ± 2 clock-tick between riders' internal clock and the common clock and this difference can change from fill to fill.
For this reason if a signal reaches all the crystals simultaneously, at the end of the reading process the signal is not synchronous anymore and a calibration is needed to obtain a sub-nanosecond time resolution. The idea to perform the calibration is sending, at the beginning of each muons fill, a simultaneous signal to all the crystals, measuring the time differences between a certain crystal and a reference one (due to the SiPM reading system) and then subtract them from the real signals. This is one of the goals of the laser calibration system.

ii. Structure of the Laser Calibration System

The geometry of the implemented laser calibration system is shown in Figure 1 [2]. The Laser Control Board provides a trigger signal that go to a NIM crate that after same logic[3] sends six outputs to the Sepia-II driver. This drives the six laser heads (pulsed diode laser) and the produced light of each one is divided in 4 parts, coupled into launching fibers (approximatively 25 m long) and sent to calorimeters. In each

[1] 54 crystals for each of the 24 calorimeters, for a total of 1296 crystals.

[2] A resolution better than a clock tick (1.25 ns) is possible because a fit of the signal wave form is performed, the reachable timing resolution is ~ 50 ps.

[3] This is needed for other calibration purpose.

calorimeter there is a secondary distribution point: the fiber encounter a diffuser that spread the light (almost) evenly to a bundle of ~ 60 smaller fibers[4].

These fibers finally send the light to each one of the crystals through a set of reflecting prisms mounted on a panel. Due to the mechanical structure of the system, the 54 fibers are in three groups of different length: approximatively 45-55-65 cm. The light gets then detected by the SiPMs and the signals are sent to the waveform digitizer via HDMI cables.

As it is clear from this structure the light does not reach the crystals simultaneously as desired for the calibration: when a laser trigger is fired the delays between the various channel are the sum of delay due to the SiPM reading system δ_R (that is what we want to know) and the ones due to different electronic and optical path in the laser system δ_C (C stand for calibration). If δ_C was known we could take it away and get δ_R. Measuring δ_C is the main task of the firt part of my project: in a way we are calibrating the calibration system!

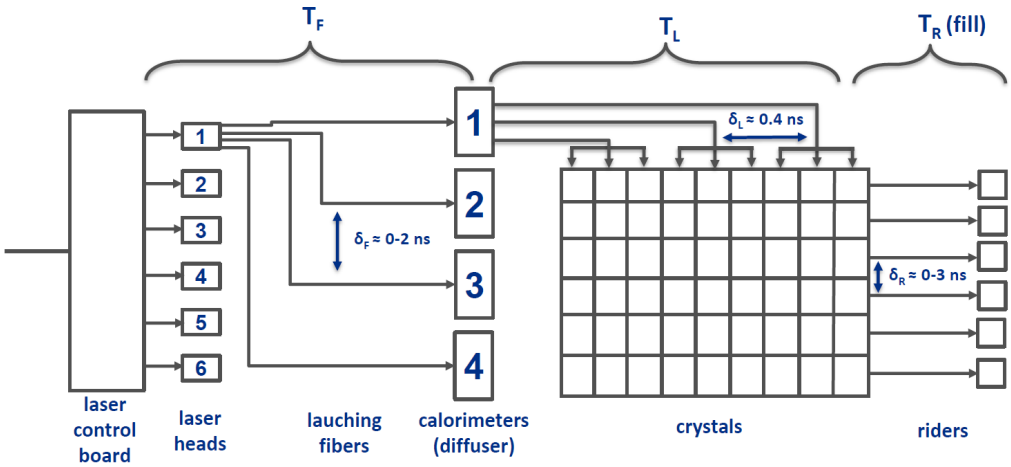

Figure 1: *A scheme of the laser calibration system with relative delay.*

[4]There are some spare one used to monitor the system.

iii. Calibration of the Laser Calibration System

Let's make same definition that will be useful in the following:

- I always identify calorimeters with index c that goes from 0 to 23. In each calorimeter, a crystal is identified by the index n that goes from 1 to 54. The mapping function between numbers and actual crystal is the standard one used in the experiment but sometimes for a better plot visualization it will be useful to use other kind of enumeration. I chose a reference calorimeter c_r and a reference crystals n_r in each calorimeters. My choice is to take calorimeter 22 and crystal 22 as references, the reason for this will be clarified later. With index f we will indicate fill number.
- With a capital T I will indicate absolute time measure by the experiment and saved by the SiPM reading system, while with the small t we will indicate time interval. With δ I mean a time differences with respect to a reference channel.
- $t_{TOT}(c, n, f)$: the time between the laser trigger and when the signal of the SiPM n of the calorimeter c is digitized in the fill f. This can be divided in 3 parts that follow.
- $t_F(c)$: the time between when the trigger is fired and when light reaches the diffuser in calorimeter c (of course this time is equal for all the crystal in a given calorimeter). This time includes the delay due to the NIM logic, which is different from one laser head to the others with differences expected to be of the order of some nanoseconds, and the time necessary for light to go through the optical path (on the optical table and through the launching fibers), which can be slightly different for the small differences in the optical path length. If plotted, these 24 times are expected to distribute in 6 groups of 4, corresponding to the laser heads.
- $t_B(c, n)$: the time between when the light reaches the diffuser in calorimeter c and when it reaches the SiPM n of that calorimeter. This is the time necessary for light to travel through the fiber bundle and through the crystal. As the fibers in the bundles are present in groups of three different lenght there will be a big difference in time for crystal connect to fibers of different length. A certain difference in time is expected as well for SiPMs connected to fibers of the same length, because these fibers are hand cutted and there could be differcies in the optical coupling at the

diffuser level. If plotted, these 54 times (for a given calorimeter) are expected to distribuite in 3 groups, corresponding to the three different lenghts in the fiber bundle.

- $t_R(c, n, f)$: the time between when light reaches the SiPM n in the calorimeter c (in the fill f) and when the signal is digitalized. The differences among this times is what we are interested in measuring and can change fill by fill. A difference in time could be seen between SiPMs connected to different riders boards.
- $t_C(c, n)$: this is the time between when the laser is triggered and when light reach the SiPM of the crystals n in the calorimeter c, e.g. the sum of $t_F(c)$ and $t_B(c, n)$
- $\delta_R(c, n, f) \equiv t_R(c, n, f) - t_R(c_r, n_r, f)$: this is what we need to synchronize signals that reach simultaneously the crystals.
- $\delta_F(c) \equiv t_F(c) - t_F(c_r)$.
- $\delta_B(c, n) \equiv t_B(c, n) - t_B(c_r, n_r)$.
- $\delta_C(c, n) \equiv \delta_F(c) + \delta_B(c, n)$: this is the delay between a generic crystal n in a generic calorimeter c and the reference crystal n_r in the reference calorimeter c_r, measuring this quantity for all the crystals is the goal of this calibration.
- $\delta_1(c) \equiv t_C(c, n_r) - t_C(c_r, n_r) = t_F(c) + t_B(c, n_r) - t_F(c_r) - t_B(c_r, n_r) = \delta_F(c) + \delta_B(c, n_r)$: this is the delay between the reference crystals n_r of the calorimeter c and the reference crystal n_r in the reference calorimeter c_r.
- $\delta_2(c, n) \equiv t_C(c, n) - t_C(c, n_r) = t_B(c, n) - t_B(c, n_r)$: this is the delay between a crystal in the calorimeter c and the reference crystal n_r of that calorimeter. Note that $\delta_C(c, n) = \delta_1(c) + \delta_2(c, n)$.
- $T_{SYNC}(c, n, f)$: at the beginning of every fill the laser is triggered, this is the absolute time saved by the reading system of the SiPM n in the calorimeter c at the fill number f associated at the laser event. The laser light reaches all the crystals at the beginning of every fill so there is a registered time for every c, n ad f.
- $T_{e^+}(c, n, f, p)$: this is the absolute time saved by the reading system of the SiPM n in the calorimeter c at the fill number f associated to a positron event p. The same positron can hit more than one crystal but always in the same calorimeter (and of course in the same fill). The ensemble of all the crystal activated by the same positron is called "cluster".

- $T_\mu(c, n, f, m)$: this is the absolute time saved by the reading system of the SiPM n in the calorimeter c at the fill number f associated at a lost muon event m. The same muon can hit more than one crystal in more than one calorimeter (of course in the same fill).

When the laser is triggered at the end of the reading process we get $T_{SYNC}(c, n, f)$ and we can compute:

$$\begin{aligned}\delta_{TOT} &= T_{SYNC}(c, n, f) - T_{SYNC}(c_r, n_r, f) \\ &= t_{TOT}(c, n, f) - t_{TOT}(c_r, n_r, f) \\ &= [t_F(c) + t_B(c, n) + t_R(c, n, f)] - [t_F(c_r) + t_B(c_r, n_r) + t_R(c_n, n_r, f)] \\ &= \delta_C(c, n) + \delta_R(c, n, f) = \delta_1(c) + \delta_2(c, n) + \delta_R(c, n, f).\end{aligned}$$

So the goal of this calibration is to measure $\delta_C(c, n)$ for all the crystals in each calorimeters. To reach this goal we will measure $\delta_1(c)$ and $\delta_2(c, n)$ separately.

What we need is an actually simultaneous signal (or something with a well-known delay) in order to calibrate the laser calibration system that is not synchronous. Example of this kind of signals are the ones produces by positrons and lost muons.

iv. Calibration via positron events

Let's consider a positron that hits more than one crystals (this can happens only for crystals in the same calorimeter). We assume that signals from positron showers reach all involved SiPMs at the same time. This statement is correct at the level of $\sim 100\,\text{ps}$ [3].

$$\begin{aligned}T_{e^+}(c, n_1, f, p) - T_{e^+}(c, n_2, f, p) &= t_R(c, n_1, f) - t_R(c, n_2, f) \\ &= t_R(c, n_1, f) - t_R(c, n_2, f) + t_R(c, n_R, f) - t_R(c, n_R, f) \\ &= \delta_R(c, n_1, f) - \delta_R(c, n_2, f).\end{aligned}$$

In the absence of reading noise if we have at least a positron event for each crystals that produces signals in at least another crystal we could find each δ_R without any need of calibration system. However δ_R can change in time, because sometimes the digitizers start counting at slight different times (± 2 clock ticks), but they are constant within a fill.

In a single fill there are not enough event for this kind of calibration but we can use this simultaneous events for the laser calibration. If instead of $T_{e^+}(c, n_1, f, p)$ we consider $t_{e^+}(c, n_1, f, p) \equiv T_{e^+}(c, n_1, f, p) - T_{SYNC}(c, n_1, f)$ we get:

$$\begin{aligned}
\delta_{e^+}(n_1, n_2) &\equiv t_{e^+}(c, n_1, f, p) - t_{e^+}(c, n_2, f, p) \\
&= [T_{e^+}(c, n_1, f, p)] - T_{SYNC}(c, n_1, f)] - [T_{e^+}(c, n_2, f, p) - T_{SYNC}(c, n_1, f)] \\
&= [T_{SYNC}(c, n_2, f) - T_{SYNC}(c, n_1, f)] - [T_{e^+}(c, n_2, f, p) - T_{e^+}(c, n_1, f, p)] \\
&= [t_C(c, n_2) + t_R(c, n_2) - t_C(c, n_1) - t_R(c, n_1)] - [t_R(c, n_2, f) - t_R(c, n_1, f)] \\
&= [\delta_C(c, n_2) - \delta_C(c, n_1) + \delta_R(c, n_2) - \delta_R(c, n_1)] - [\delta_R(c, n_2) - \delta_R(c, n_1)] \\
&= \delta_C(c, n_2) - \delta_C(c, n_1).
\end{aligned} \tag{3}$$

δ_C do not change in time so one can easily accumulate enough positron events till they links together all the crystals in a calorimeter. With positron event we can link only crystals in the same calorimeter so:

$$\delta_C(c, n_2) - \delta_C(c, n_1) = \delta_1(c) + \delta_2(c, n_2) - \delta_1(c) - \delta_2(c, n_1) = \delta_2(c, n_1) - \delta_2(c, n_2). \tag{4}$$

With this kind of signal we can only compute δ_2. To get δ_C (or equivalently δ_1) we need signals that reach crystals on different calorimeters at the same time or with a knowable time interval (for example the signal produces by lost muons that cross two or three calorimeters).

Let's compute the only δ_2, we still have to deal with the noise: all the time measurement have a certain resolution and consequently a certain error.

Let's define

$$t^*_{e^+}(c, n, f, p) \equiv T^*_{e^+}(c, n, f, p) - T_{SYNC}(c, n, f)$$

where $T^*_{e^+}(c, n, f, p)$ is the "true" time, i.e. unaffected by the noise.

Starting from this quantity and by Equation 3 and Equation 4. I can define:

$$t^*_{e^+}(p) = t^*_{e^+}(c, n_r, f, p) \equiv t^*_{e^+}(c, n, f, p) - \delta_2(c, n). \tag{5}$$

This a fictitious quantity, in the sense that it is not measurable because in general the shower generated by positron p will not cross the reference crystal n_r.

The reading noise will essentially be the time resolution $\sigma_{c,n}$ which in principal should depend only on the SiPM and in first approximation will be equal for the SiPM. So we need to perform a fit, let's evaluate this χ^2:

$$\chi^2 = \sum_{p}^{n_{e^+}} \sum_{n} \frac{[t^*_{e^+}(p) + \delta_2(c,n) - t_{e^+}(c,n,f,p)]^2}{\sigma^2_{c,n}}. \tag{6}$$

Here the calorimeter c is fixed and all the considered positron event are on this calorimeter. In this expression I'm summing over all the n_{e^+} selected positron event p and for each one I'm summing over all (or a selection of) the crystal n where the positron produce a signal. Of course I'm considering only positron event that produce signal in two or more crystals, because positron that hit a single crystal give no information on timing. In this expression $t_{e^+}(c,n,f,p)$ are the measured quantities and the unknowns are the n_{e^+} $t^*_{e^+}(p)$ and the 53 $\delta_2(c,n)$ (remember that c is fixed and that $\delta_2(c,n_r) \equiv 0$.

We can find these unknowns minimizing the χ^2 function:

$$\frac{\partial \chi^2}{\partial \delta_2(c,n)} = 0 \rightarrow \sum_{p} t^*_{e^+}(p) + N_n \delta_2(c,n) = \sum_{p} t_{e^+}(c,n,f,p) \qquad \text{(53 equation)}$$

$$\frac{\partial \chi^2}{\partial t^*_{e^+}(p)} = 0 \rightarrow N_{e^+} t^*_{e^+}(p) + \sum_{n} \delta_2(c,n) = \sum_{n} t_{e^+}(c,n,f,p) \qquad (n_{e^+} \text{ equation})$$

where N_n is the number of times that the crystal n (in calorimeter c) is hit by all the selected positron events, and N_{e^+} is the number of (selected) crystals hit by a single positron event. We then have a set of $53 + n_{e^+}$ linear equations and the same number of unknowns so linear system is solvable.

iv.1 Positron selection and result

We choose crystal 22 as reference crystal because it is one of the central ones and this is convenient from a statistical point of view. Due to statistical and computational reasons, we highly filter the data set so that for each calorimeter each crystal appears in at least 500 clusters and the overall number of equations is around 15000. This enormous linear system can be considered as a square matrix, that happens to be symmetrical, mostly diagonal and very sparse. To solve this system, a matrix inversion is computationally

prohibitive, since it scales roughly as $O(n^3)$. The `ROOT` class `TMatrixDSparse`, built specifically to handle this kind of matrices, helps to solve this very quickly.

This method finds all the $\delta_2(c,n)$ at once but it is limited by the dimensions of the matrix. To select only quality event suitable for the calibration we make a cut in energy in the single crystal (more than 300 MeV) and cluster energy (more than 1 GeV).

In Figure 2 we can see in red the result for an example calorimeter. In this plot the crystals are column enumerated: in this way it is clear the structure in 3 groups, corresponding to the different lengths of the fiber in the bundle from the diffuser. In black I report for comparison the result via a different technique as exposed in [4].

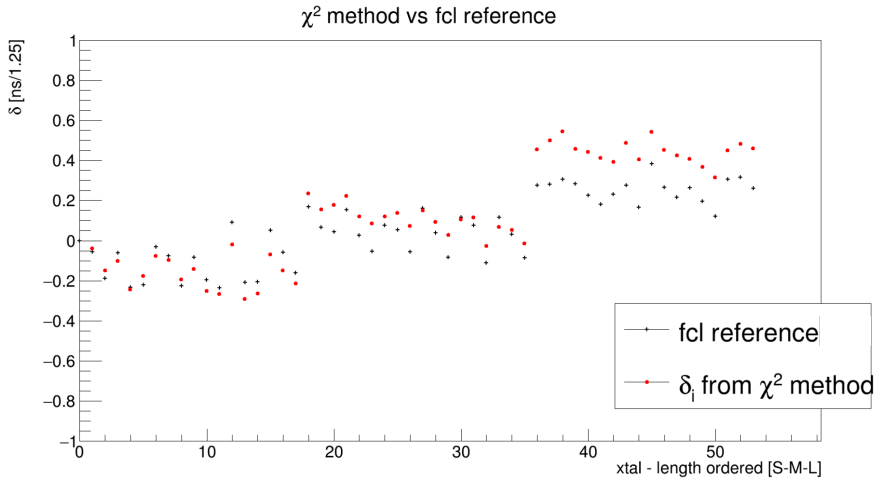

Figure 2: *In red, the fitted δ_2 for calorimeter 10 using χ^2 method on the positron events. In black the result of a calibration made by a different technique [4]*

There are same discrepancies and the reason could be the energy selection: in Figure 3 the fit is repeated for different energy selection and what we see is a clear trend. Maybe the assumption that positron signals is synchronous int he SiPMs is not sufficiently good.

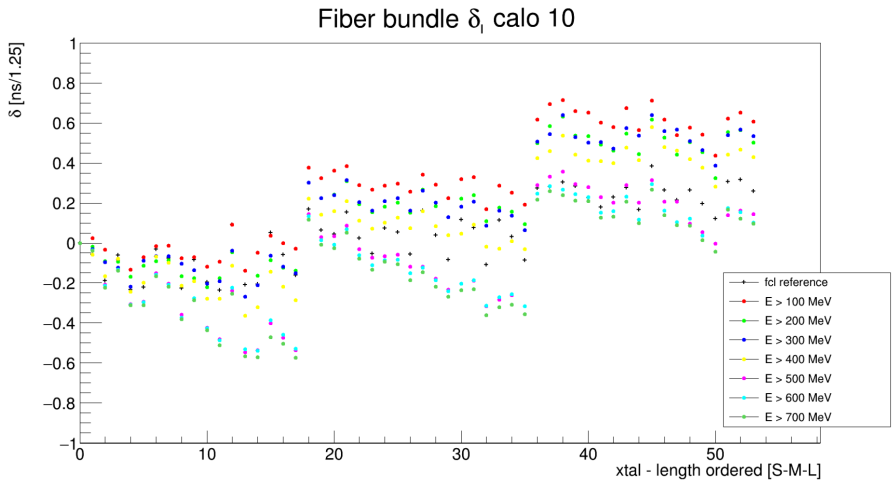

Figure 3: *Fitted δ_2 for calorimeter 10 using χ^2 method on the positron events for many different energy selection.*

v. Calibration via lost muon events

Let's consider now a muon that is lost from the accumulation ring and that cross two (or more) calorimeter. Clearly in this case the signal on the two different calorimeters cannot be considered simultaneous anymore because these are a couple of meters away which means a delay $t_{TOF}(c_1, n_1, c_2, n_2) \simeq 6/7\,\text{ns}$.

The time of flight in first approximation depends only on the calorimeter and not on the specific crystal because calorimeters dimensions are negligible compared to the distance between them, so we have $t_{TOF}(c_1, n_1, c_2, n_2) \simeq t_{TOF}(c_1, c_2)$.

Similarly to the positron case we define

$$t_\mu(c_1, n_1, f, m) = T_\mu(c, n_1, f, m) - T_{SYNC}(c_1, n_1, f)$$

and consequently:

$$\begin{aligned}
\delta_\mu(c_1,n_1,c_2,n_2) &\equiv t_\mu(c_1,n_1,f,m) - t_\mu(c_2,n_2,f,m) \qquad (7)\\
&= [T_\mu(c_1,n_1,f,m)] - T_{SYNC}(c_1,n_1,f)] - [T_\mu(c_2,n_2,f,m) - T_{SYNC}(c_2,n_2,f)]\\
&= [T_{SYNC}(c_2,n_2,f) - T_{SYNC}(c_1,n_1,f)] - [T_\mu(c_2,n_2,f,m) - T_\mu(c_1,n_1,f,m)]\\
&= [t_C(c_2,n_2) + t_R(c_2,n_2) - t_C(c_1,n_1) - t_R(c_1,n_1)]\\
&\quad - [t_{TOF}(c_1,c_2) + t_R(c_2,n_2,f) - t_R(c_1,n_1,f)]\\
&= [\delta_C(c_2,n_2) - \delta_C(c_1,n_1) + \delta_R(c_2,n_2) - \delta_R(c_1,n_1)]\\
&\quad - [t_{TOF}(c_1,c_2) + \delta_R(c_2,n_2) - \delta_R(c_1,n_1)]\\
&= t_{TOF}(c_1,c_2) + \delta_C(c_2,n_2) - \delta_C(c_1,n_1)\\
&= t_{TOF}(c_1,c_2) + \delta_1(c_2) + \delta_2(c_2,n_2) - \delta_1(c_1) - \delta_2(c_1,n_1).
\end{aligned}$$

We now have two options:

- if we have enough lost muons that cross through all the crystals we can in principle compute directly all the $\delta_C(c,n)$, however this is not the path we will travel, even if it is feasible;
- from the previous calibration with the positron we already know all the $\delta_2(c,n)$ so we can subtract them to obtain the $\delta_1(c)$.

We can apply a similar strategy to the one used to compute $\delta_2(c,n)$. Let's define:

$$t^*_\mu(c,n,f,m) \equiv T^*_\mu(c,n,f,m) - T_{SYNC}(c_r,n_r,f)$$

where $T^*_\mu(c,n,f,m)$ is the "true" time, i.e. unaffected by the noise.

Starting from this quantity and from Equation 7:

$$T^*_\mu(m) = T_\mu * (c,n,f,m) + \Delta c \cdot t_{TOF} - \delta_1(c)$$

where t_{TOF} is the time needed for the muon to travel from a calorimeter to the next one (here we are approximating all the calorimeter at the same exactly distance) and Δc is the distance from the reference calorimeter in calorimeter unit (modulus 24).

This is a fictitious quantity: it is measurable only if the muon cross the reference calorimeter, in the other cases we have to imagine that this muons his traveling along a polygonal path from a calorimeter to the next one in straight line.

The reading noise will essentially be the time resolution $\sigma_{c,n}$ which in principle should depend only on the SiPM and in first approximation will be equal for the SiPM. Let's evaluate this χ^2: [5]

$$\chi^2 = \sum_{m}^{n_\mu} \sum_{c} \frac{[t^*_\mu(m) - \delta_2(c,n) - t_{e^+}(c,n,f,p) - \Delta c \cdot t_{TOF} - \delta_1(c)]^2}{\sigma^2_{c,n}} \tag{8}$$

In this expression I'm summing over all the n_μ selected muon event m and for each one I'm summing over the calorimeters c that the muon cross producing a signal. Practically we can have only signal in two or three calorimeter. If a muon produce signal in more than one crystal in the same calorimeter I should also sum on it but in the following we will consider only muon that hit a single crystal per calorimeter.

Of course I'm considering only muon event that produce signal in two or more calorimeter, because muon that cross a single calorimeter give no information on timing between different calorimeters (they gives timing information for crystal among the same calorimeter, exactly like the positron).

In this expression $t_\mu(c,n,f,p)$ are the measured quantities, $\delta_2(c,n)$ are constant known by the previous calibration passage via positron event and the unknowns are the $t^*_\mu(m)$ (n_μ in number), the 23 $\delta_1(c)$ (remember that $\delta_1(c_r) \equiv 0$) and t_{TOF}[5]. We can find these unknowns minimizing the χ^2 function exactly like in the previous section solving a system of $(n_\mu + 23 + 1)$ equation.

v.1 Muon selection and result

I choose calorimeter 22 as reference calorimeter just to uniform to [4].

In this analysis only two calorimeter events are selected, with only one crystal hit per calorimeter, and an energy cut of 120 MeV $< E_{hit} <$ 220 MeV applied: this is centered on the energy that a MIP muon release in a E989 crystal ($\sim$ 170 MeV).

The time cut has been left very broad, i.e. $\Delta t <$ 30 ns, since the measured times have to be corrected for the sync pulse as described above. In the selection of events we indeed have some background, e.g. low-energy positrons misidentified as muons, or two independent muons hitting in the coincidence windows.

[5] Remarkably in this approach this is a fittable parameter and there is no need to esteem in other ways.

In Figure 4 the result of this analysis is shown for different run spaced in time to verify stability in time. It is clear a structure of 6 group of 4 calorimeters, each corresponding to a different laser head.

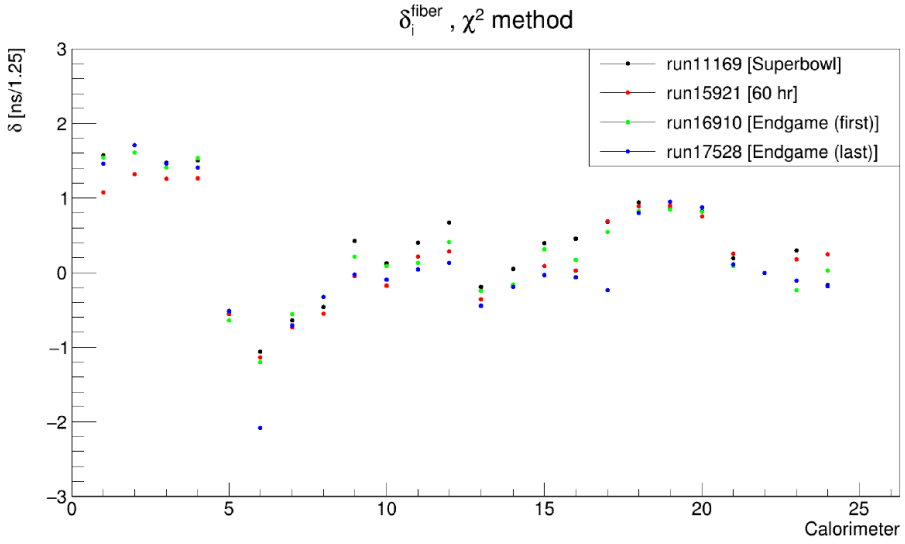

Figure 4: *Fitted δ_1 using χ^2 method on the lost muons events different runs spaced in time.*

vi. Calibration via hardware measurement

There is an other way to perform the $\delta_1(c)$ measurement with a direct hardware measurement [2]. Let's consider an experimental setup like outlined in Figure 5.

Each calorimeter is equipped with a probe fiber (one of the spare connected to the diffure) that has an open end. By connecting the probes of two different calorimeters to a PMT, we can monitor the arrival times of the same laser pulse with an oscilloscope and actually measure something the is really similar to δ_F which is an approximation of δ_1.

In our setup (see Figure 7) the PMT is connected directly to the probe of the calorimeter 24. The other calorimeters' probe is reached using a 20 m long fiber. The time difference between the two peaks observed in the oscilloscope represent the time the light needs to travel the 20 meters (that is always the same) plus the $\delta_F(c) - \delta_F(24)$ and

plus $\delta_P(c)$ which is the time difference due to the different length of the probe fiber which vary in length at the order of 1 cm, that mean $\sim 50ps$.

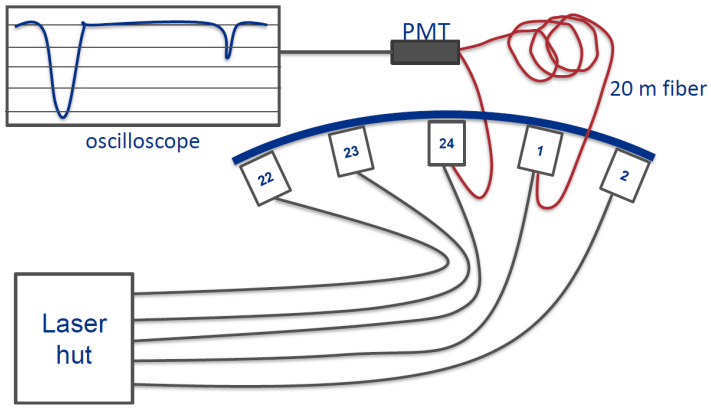

Figure 5: *Scheme of the setup for the hardware measurement of the* $delta_1(c)$

For each calorimeter we recorded 500 waveforms, and after fitting every peak with a parabola, we obtain a distribution of the time difference between the peaks. An example of typical waveforms and relative fit is presented in Figure 6.

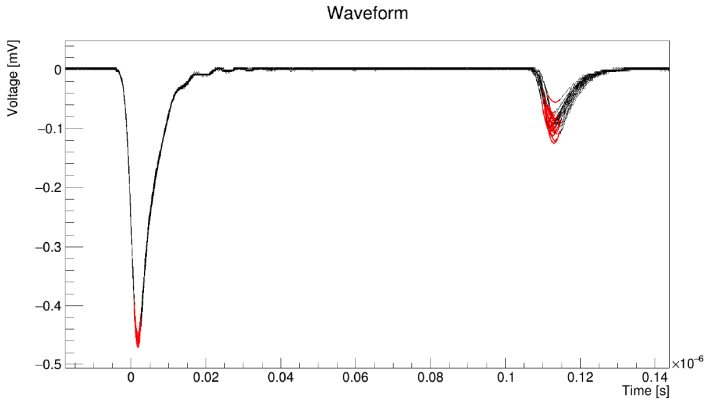

Figure 6: *An example of the waveforms registered by the oscilloscope. Parabolic fits are performed for both peaks, here shown in red.*

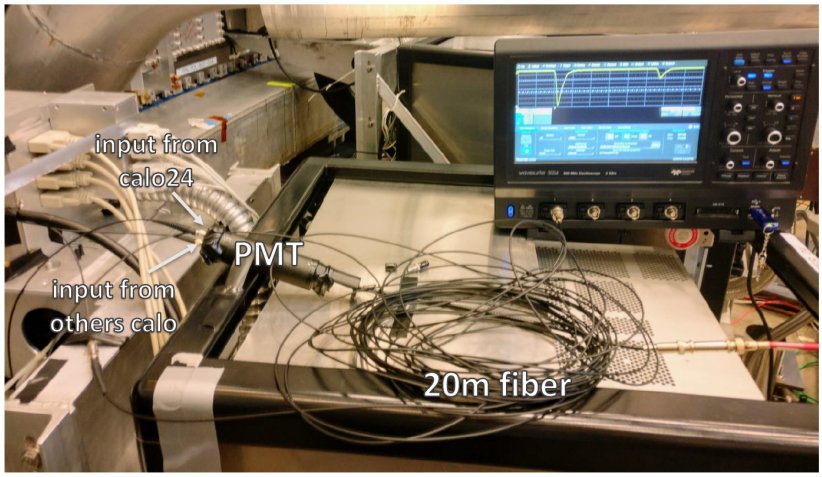

Figure 7: *Photo of the actual setup used in the calibration*

One possible systematic error of this analysis comes from the amplitude of the PMT signal. A larger pulse could systematically shift the fitted time. To test whether this is relevant or not, we repeated the measurement of calorimeter 1 five times, changing the intensity of the laser via the corresponding filter wheel. What we found is a difference of the order of 50 ps and for safety we decide to take count of this effect during the data taking modifying the laser intensity case by case.

It is important to notice that what we are measuring is $\delta_F(c) + \delta_P(c)$ but we are interested in $\delta_1(c) = \delta_F(c) + \delta_B(c, n_r)$. $\delta_B(c, n_r)$ depends on the difference in the lengths of the small fibers (in the bundle from the diffuser) between the reference crystal in the reference calorimeter and the reference crystal in the calorimeter c that should be at the order of 1 cm, that mean ~ 50 ps.

In Figure 8 we can see the result of the measurement made at two different times: at the begin and at the end of the summer school. There are same big differences because some hardware changes were made in the electronic connection between the Laser Control Board and the laser head.

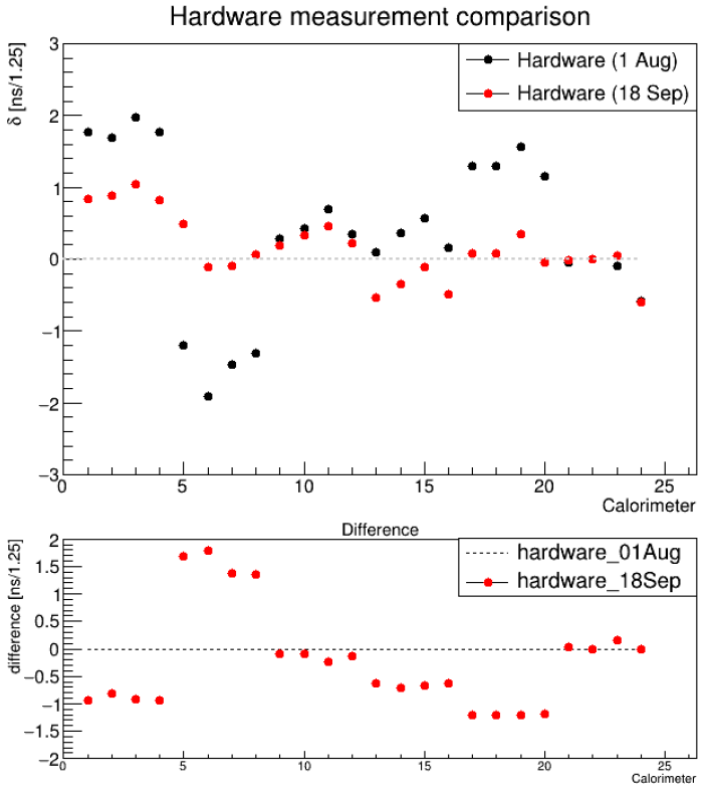

Figure 8: *Comparison between two different δ_2 hardware measurement made at the start and finish of the summer school. In the meanwhile some hardware changes were made at the NIM crate.*

vi.1 Result and comparison

In Figure 9 is reported the comparison between the reference in [4] made with a different technique (in red), the result of the chi^2 method (in black) and the result of the hardware measurement (in green). There is a big divergence between the hardware measurement and the other two methods: this could be possible if same changes in the electronic in the laser hut has been made between the run and the hardware measurement but it is not clear.

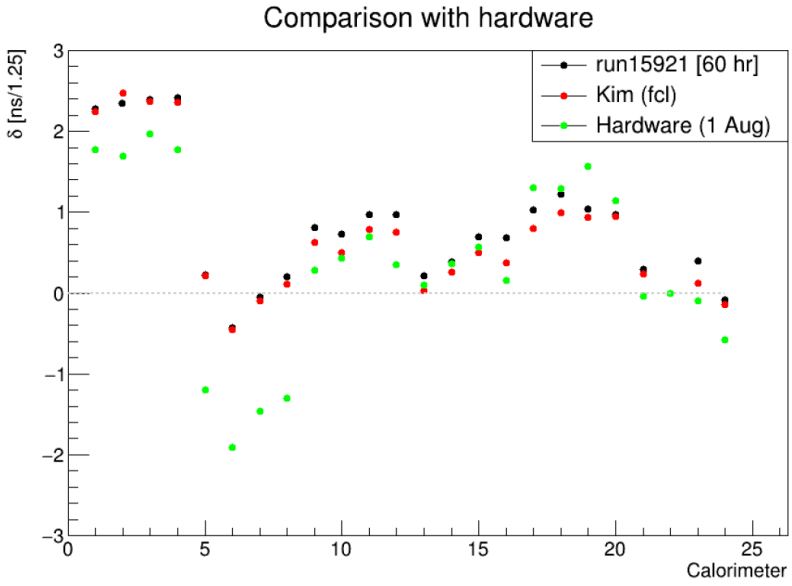

Figure 9

vii. Conclusion

The energy dependency in δ_2 fit seems to be a big problem for the validity of the method, however δ_2 is small compared to δ_1.

The only way to dissipate doubts on the validity of the hardware measurement is to wait another run and perform the software calibration on the data.

III. A preliminary study of the energy binned wiggle fit

i. Introduction

In this experiment the polarized positive muons are stored in a magnetic ring. Their spins precess at a different rate than their momenta. The anomalous precession frequency ω_a is the difference between the ensemble-averaged muon spin precession and cyclotron frequencies.

Direct measurement of the muon spin is not practicable so an indirect measurement is made via the decay positrons. Muon decay proceeds through the weak force and therefore is parity violating.

The consequence of this behavior is that the emitted positron momentum is correlated with the muon spin direction. Therefore by measuring the decay positrons and analyzing their energies, a measurement of the muon spin is possible.

The rate of detected positrons above a single energy threshold E_{th} is

$$\frac{dN(t; E_{th})}{dt} = N_0 e^{-t/\gamma\tau_\mu}[1 + A\cos(\omega_a t + \phi)]. \tag{9}$$

Here the normalization, N_0, average asymmetry A and initial phase *phi* are all dependent on the threshold energy. A parameterization of this function is used to fit the results from the T-method analysis and extract ω_a.

However it is possible to extract more statistical precision from the data set. The information of the muon spin is encoded via the positron momentum. By weighting events in proportion to their energy, or the asymmetry associated with their energy, the statistical precision is improved.

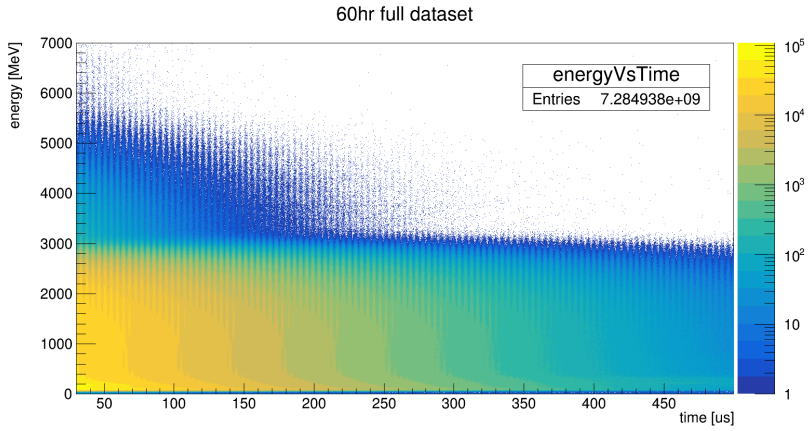

Figure 10: *2D histogram: energy vs time of the fill. This is the starting point of every ω_a fitting technique.*

The starting point for every kind of ω_a analyses is this 2D histogram energy vs time of the fill. This was already produced by the reading software in ω_a-Europa group as a debugging tool for single calorimeters and it is now produced for all calorimeters.

All the work I performed was on the new full 60hr dataset. From this plot we can catch some of the key correction one should apply in order to do a proper fit: pileup in the region above 3.1 GeV and lost muons (in the first microseconds) around the MIP energy. From this histogram one can performs every possible analyses.

ii. The T-method fit

The standard analysis procedure is to identify individual decay positrons and plot the rate of their arrival versus time using only events having a measured energy above a threshold. This method is named the T (time) method. It was the dominant analysis technique used in the Brookhaven experiment and it is well tested against systematic errors.

For example in the plot in Figure 11 I integrate all signals above 1.7 GeV and then fitted the time dependence with a 5 parameter fitting function:

$$N(t) = N_0 e^{-t/\tau}[1 + A\cos(\omega_a t + \phi)]. \tag{10}$$

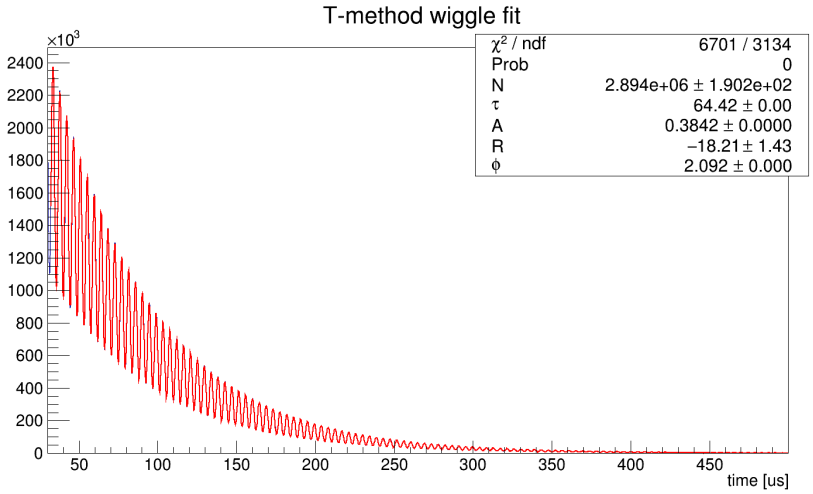

Figure 11: *Wiggle plot for all the event above the threshold of 1.7 GeV.*

The free parameter in this kind of analyses is the threshold value. To understand the maximum statistic power of this method I computed the T-method for many threshold from 0 to 3 GeV and plotted the result for R, that is a blinded quantity for ω_a ($d\omega_a/\omega_a$). The bigger error for high energy threshold is due to low statistic, while the values for low energy threshold are due to lost muon, because MIP muons in these kind of crystal have energy near 170 MeV.

For each energy threshold a 5 parameters fit has been performed. In Figure 12 is reported the plot of the errors on the fitted R versus the energy threshold. We can see a very clear trend with a minimum around 1.7 GeV and an error of 1.43 ppm, with a growing trends at high energy due to decreasing statistic and the same phenomenon at low energy due to the decreasing asymmetry. That is because asymmetry in the decay positron is energy dependent and as we'll se later it is zero around 1 GeV, positive for higher energies and negative (and small) for lower energies.

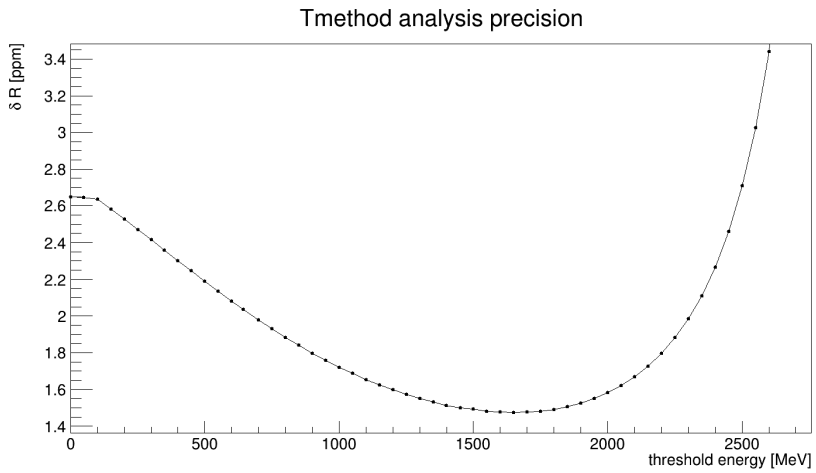

Figure 12: *T-method precision versus energy threshold. The maximum is reached for a threshold near 1.7 Gev and for this dataset*

iii. The Energy binned fit

The aim of this section is to discuss a relatively new [6] fitting method: the energy binned fit method: the idea is to take slices of the 2D histogram in Figure 10: that is dived this plot in energy bin, integrate and than fit w_a in each bin. In Figure 13 there are examples of what one gets. It is clear the asymmetry dependency on energy.

Asymmetry dependency In Figure 14 we can see the fitted asymmetry versus the central energy: for energy near 1 GeV the asymmetry is nearly 0 and for lower energies it became negative. In fact if we compare the wiggle plot of the 400-600 MeV bin and the others above 1 GeV (let's say 1200-1400 MeV) we'll see that it seems like a difference of π in the phase, it is indeed a change in the sign of A.

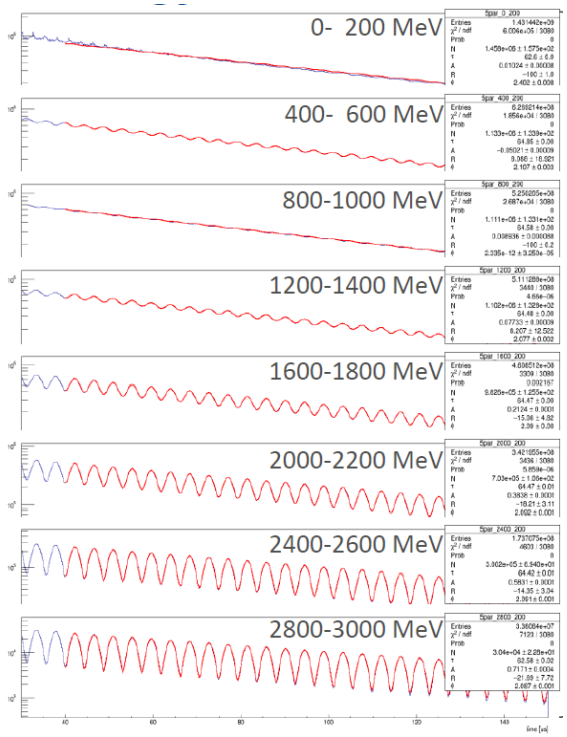

Figure 13: *Wiggle plot for different energy bin. It is cealr the asymmetry dependency.*

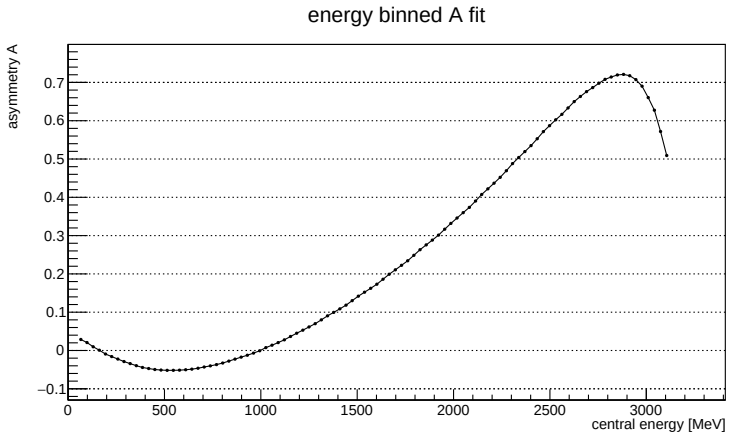

Figure 14: *Fitted asymmetry A vs central energy of the bin.*

When the fit in each bin as been performed we can plot all the results and compute a constant[6] fit, weighting every fitted R with his standard deviation. The result is showed in Figure 15.

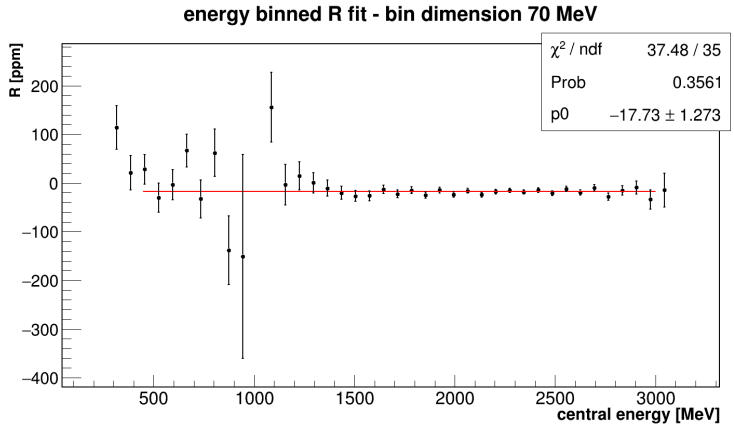

Figure 15: *Energy binned fit with a bin dimension of 70 MeV. Every point is a 5 parameter fit with uncorrected data from the 60hr dataset.*

This is the result of the energy binned method made with the 5 parameters fit and with a bin dimension of 70 MeV: I decide to fit using energy bin between 500 and 3000 MeV because:

- points at low energy have some problem due to the lost muons that populate the MIP bin, root minimization routine fail and do not converge;
- points with high energy, over 3 GeV have big errors due to low statistic and often fit have problem in convergence.

In this fitting technique the bin dimension (and consequently bin number) is a free parameter and we expect that the statistical power of the method should asymptotically reach a constant for increasingly high number of bin. This assumption is verified in Figure 16 and it is possible to esteem an asymptotic precision of ~ 1.27 ppm with this

[6]That's because we do not expect any sort of dependency of ω_a from energy that is a property of the positron.

dataset, to be compared with the maximum precision of 1.45 ppm reachable with the T-method with the same dataset.

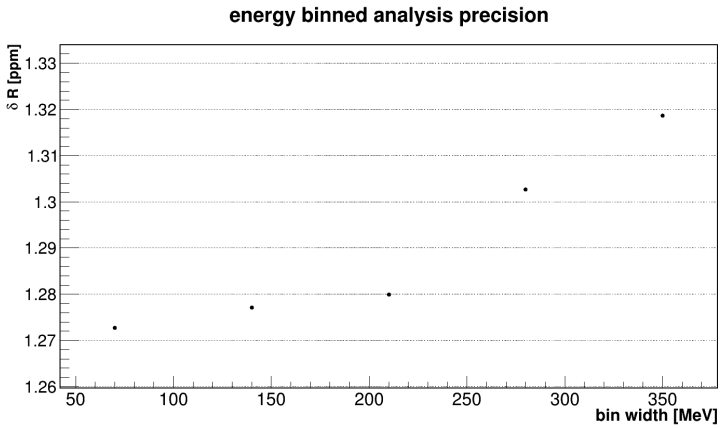

Figure 16: *Energy binned method precision vs bin dimension. Every point is a 5 parameter fit performed on uncorrected data from the 60hr dataset. An asymptotic precision of* 1.27 *ppm is reached.*

iv. Application of same correction

iv.1 CBO frequency correction

Another common fitting function is the so called 9 parameters fit:

$$N(t) = N_0 e^{-t/\tau}[1 + A\cos(\omega_a t + \phi)][1 - e^{-t/\tau_{cbo}} A_1 \cos(\omega_{cbo} t + \phi_1)] \tag{11}$$

This fit is used to take count of a spurious frequency due to the CBO (Coherent Betatron Oscillation) that produce a systematic error and poor quality fit if neglected. I tried to perform also this fit but with little success: usually for energies in the 1200-2700 MeV region the fit is successful, as we can see from the residual FFT in Figure 17 which doesn't show any pick in the CBO region, but outside this region the result is like in Figure 18, which means that the fit is failed, probably due to a poor initial parameter estimation.

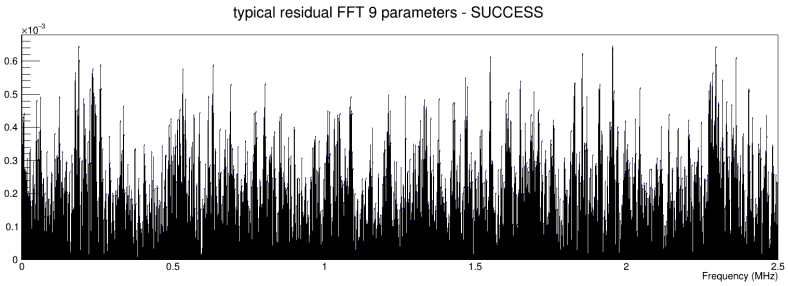

Figure 17: *FFT of a succeeded 9 parameter fit there is no visible excess at the CBO frequency.*

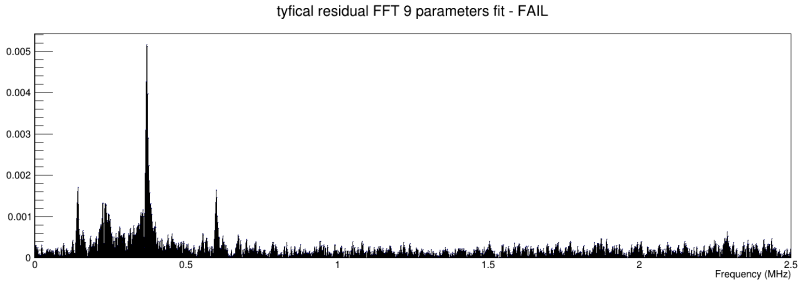

Figure 18: *FFT of a failed 9 parameter fit there is a clear excess at the CBO frequency.*

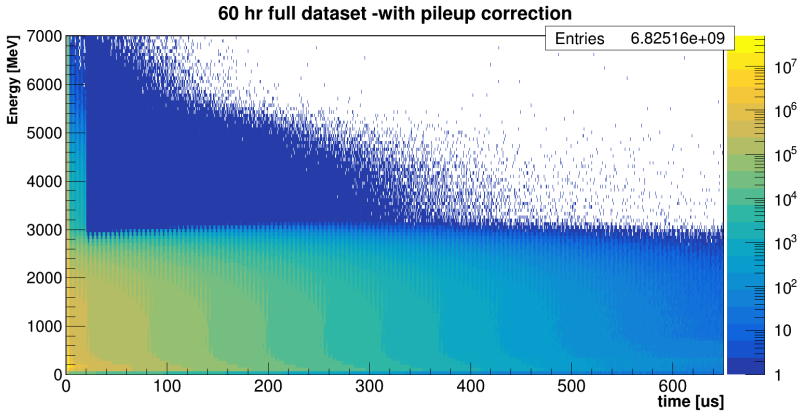

Figure 19: *These are the same data of the 2D histogram in Figure 10 but with a pile-up correction applied*

iv.2 Pile-up correction

Another important correction that is performable is the pile-up correction. I take the corrected 2D histogram in Figure 19 performed by Matthias Smith within the ω_a-Europa group and I run the energy binned fit.

The asymptotic precision reached with these corrected data and the 9 parameter fit (which however works in the region that takes more information) is near 1.05 ppm and is showed in Figure 20 which is indeed a slight improvement.

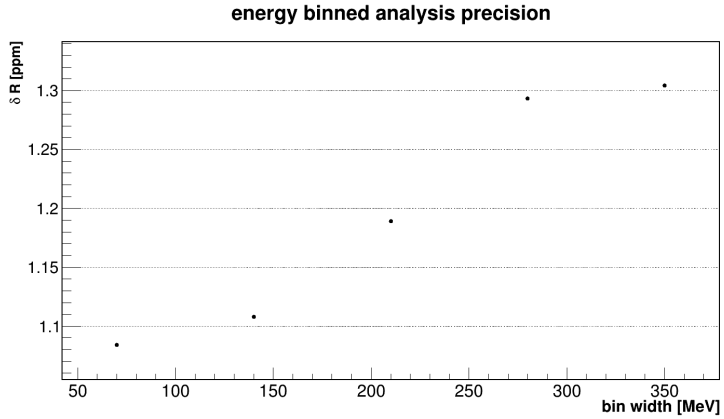

Figure 20: *Energy binned method precision vs bin dimension. Every point is a 9 parameter fit performed on pile-up corrected data from the 60hr dataset. An asymptotic precision of* 1.05 *ppm is reached.*

v. Conclusion

In conclusion the energy binned fit provides better statistical precision than T-method and that applying import correction such as CBO and pile-up can improve the situation. It is however important to perform a study of the sensitivity of this new fitting technique from the main sources of systematic error.

IV. Other works done at the experiment

During the Summer Internship other works has been performed at the experiment:

- Installation of two new optical fiber in order to distribute the laser signal to the *fiber-harp*. Thi is a diagnostic tool collocated in the ring that using a strip of scintillating fiber (a "fiber harp") is capable to identify form and position of the beam. A connection with the laser control system was needed and I helped in building the new optics on the optical table and actually install the fibers under the ring (see Figure 21).
- Connection and disconnection of same calorimeters and the laser calibration system. That's because same calorimeter need to be removed of reinstalled for maintenance. (see Figure 22).

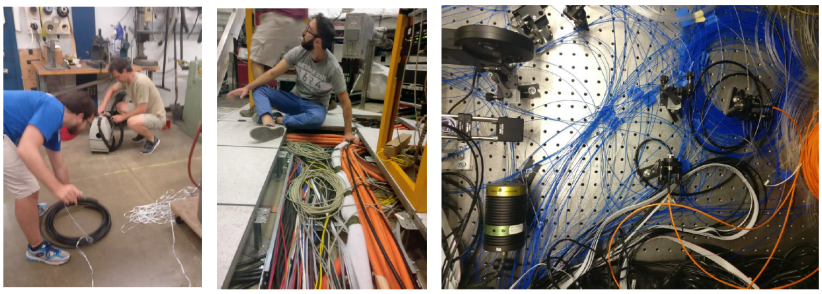

Figure 21: *Installation of two new optical fiber in order to distribute the laser signal to the fiber-harp.*

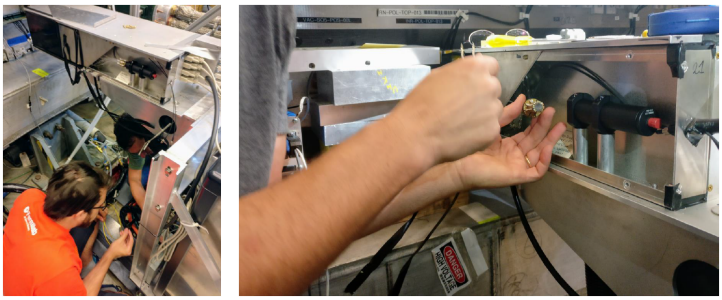

Figure 22: *Connection and disconnection of same calorimeters and the laser calibration system.*

References

[1] J. Grange et al. [Muon g-2 Collaboration], *Muon (g-2) Technical Design Report*, arXiv:1501.06858, (2015).

[2] P. Girotti et. al., *The Time Synchronization of 1296 Crystals*, G-2 Experiment Document 14851-v2, (2018).

[3] Robin Bjorkquist, *Crystal timing shift systematic study*, G-2 Experiment Document 2274-v1, (2014).

[4] K. Khaw, *Recon West update: a tale of time and energy*, G-2 Experiment Document 11055-v7, (2018).

[5] J. Stapleton, *Crystal Timing Calibration*, G-2 Experiment Document 9182-v1, (2017).

[6] A. Fienberg, *Characterization of an Energy Binned ω_a Analysis*, G-2 Experiment Document 8789-v1, (2017).